A new wrapper for a reliable resolution of underdetermined nonlinear equations

Luc Jaulin

November 5, 2025

Abstract

This paper introduces a new wrapper called a *gutter*. Gutters are used to enclose a part of the solution set defined by nonlinear equations. We show that gutters may allow us to obtain a better accuracy for the approximation with less computations. Some examples taken from the literature illustrate the efficiency and the accuracy of the approach.

1 Introduction

In this paper, we want to characterize the set

$$\mathbb{X} = \{\mathbf{x} \in [\mathbf{x}] | \mathbf{f}(\mathbf{x}) = \mathbf{0}\} \tag{1}$$

where $\mathbf{x} \in \mathbb{R}^n$ and $\mathbf{f}(\mathbf{x}) \in \mathbb{R}^m$ is a nonlinear differentiable function. We assume that $m < n$. This type of problems has already be considered by several authors using interval based methods [6][16][15][11][17][20][18]. To characterize the solution set, we can build a paving of $\mathbb{R}^n$ made with boxes. For each box $[\mathbf{x}]$ of the paving, we can compute an approximation of the solution. Moreover, if a high accuracy is required, a first order approach is needed.

Let us recall the principle of a first order approach [15][5][7], taking a small box $[\mathbf{x}]$ with center $\bar{\mathbf{x}}$, as illustrated by Figure 1.

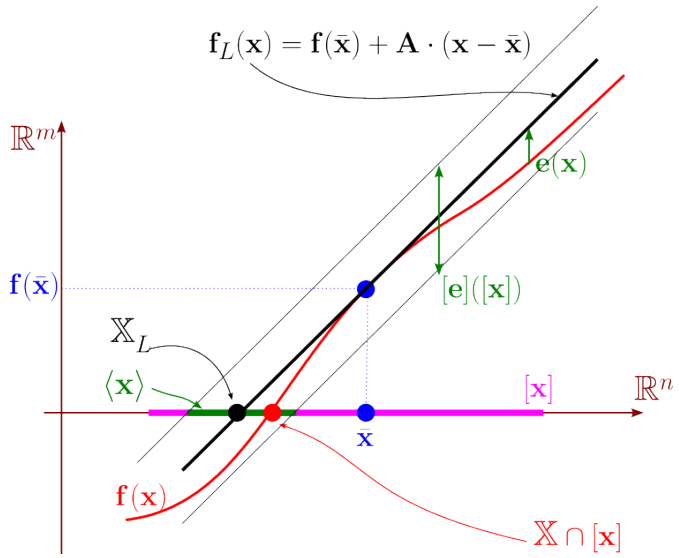

Figure 1: Principle to get $\langle \mathbf{x} \rangle$, a first order approximation of $\mathbb{X} \cap [\mathbf{x}]$

On this small box, we build the following linear approximation:

$$\mathbf{f}(\mathbf{x}) \simeq \underbrace{\mathbf{f}(\bar{\mathbf{x}}) + \mathbf{A} \cdot (\mathbf{x} - \bar{\mathbf{x}})}_{\mathbf{f}_L(\mathbf{x})} \tag{2}$$

where $\mathbf{A} = \frac{d\mathbf{f}}{d\mathbf{x}}(\bar{\mathbf{x}})$. The linear approximation set for $\mathbb{X}$:

$$\mathbb{X}_L = \{\mathbf{x} \in [\mathbf{x}] | \mathbf{f}_L(\mathbf{x}) = \mathbf{0}\} \tag{3}$$

is valid on the box $[\mathbf{x}]$. Equivalently, we can write

$$\mathbb{X} \cap [\mathbf{x}] \simeq \mathbb{X}_L \cap [\mathbf{x}] \tag{4}$$

Now, this approximation is not reliable. Indeed, if the error

$$\mathbf{e}(\mathbf{x}) = \mathbf{f}_L(\mathbf{x}) - \mathbf{f}(\mathbf{x}) \tag{5}$$

is small for all $\mathbf{x} \in [\mathbf{x}]$, we cannot conclude that $\mathbb{X} \cap [\mathbf{x}]$ and $\mathbb{X}_L \cap [\mathbf{x}]$ are close. For instance if $\mathbf{f}(\mathbf{x}) = \mathbf{0}$ for all $\mathbf{x} \in [\mathbf{x}]$ and we can always find $\mathbf{f}_L(\mathbf{x})$ (for instance, a constant) which is a good approximation for $\mathbf{f}$ but which never vanishes. However, this situation occurs only when the Jacobian of $\mathbf{f}$ is not full rank and can be considered as non-generic.

In this paper, we propose to use this first order approach to enclose the solution set $\mathbb{X}$. For this, we need to compute a reliable upper bound for the distance between the two sets $\mathbb{X} \cap [\mathbf{x}]$ and

$\mathbb{X}_L \cap [\mathbf{x}]$. More precisely, we need to know how much we need to inflate $\mathbb{X}_L$ in order to get an enclosure $\langle \mathbf{x} \rangle$ for $\mathbb{X} \cap [\mathbf{x}]$.

The notion of first order approximation is taken from [5] where an approximation of order k is said to be obtained if $\text{Vol}(\langle \mathbf{x} \rangle) = O(\varepsilon^n \cdot \varepsilon^{k(n-m)})$, where $\varepsilon = O(w([\mathbf{x}]))$, $w([\mathbf{x}])$ denoting the width of $[\mathbf{x}]$. This is illustrated by Figure 2, in the case $n = 2$, $m = 1$, $k = 1$. We have indeed $\text{Vol}(\langle \mathbf{x} \rangle) = O(\varepsilon^2 \cdot \varepsilon^{1\cdot(2-1)}) = O(\varepsilon^3)$, whereas $\text{Vol}([\mathbf{x}]) = O(\varepsilon^2)$.

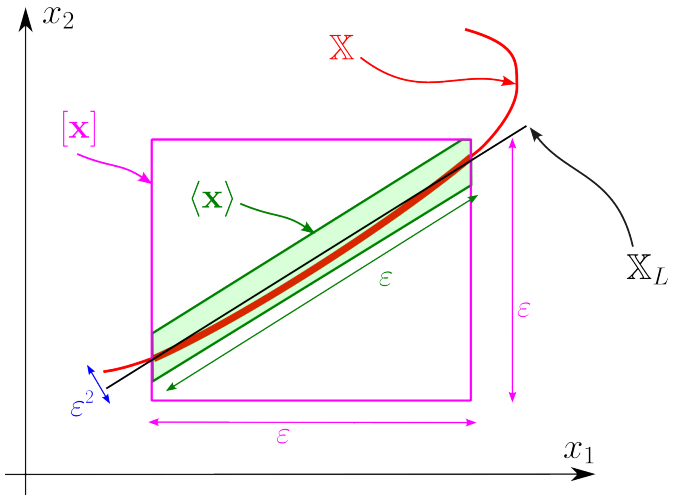

Figure 2: The set $\langle \mathbf{x} \rangle$ is a first order approximation for $\mathbb{X} \cap [\mathbf{x}]$

This paper is organized as follows. Section 2 recalls the approximation theorem needed to enclose $\mathbb{X} \cap [\mathbf{x}]$ by a polygon for a small box $[\mathbf{x}]$, *i.e.*, for a box with a small width. Section 3 introduces a new type of domain called *gutter*, which is defined by a box $[\mathbf{x}]$, an affine function $\mathbf{Ax} = \mathbf{b}$ (called a *flat*), and a radius ρ. Gutters are easy to handle (project, intersect, ...) still preserving an order one approximation. Section 4 defines the notion of gutter contractors that will be used to approximate accurately the solution set. An illustration of the efficiency of gutters is given in Section 4 on three test-cases taken from the literature. Section 6 concludes the paper.

2 Approximation theorem

This section proposes a method to compute an outer approximation of $\mathbb{X} \cap [\mathbf{x}]$ with an order one.

2.1 Parallel linearization

As written previously, to enclose $\mathbb{X} \cap [\mathbf{x}]$, we need first to enclose the graph $\mathbf{f}(\mathbf{x})$ over $[\mathbf{x}]$. This can be done using the parallel linearization (see Section 4.3.4 of [9]). For this, we approximate $\mathbf{f}(\mathbf{x})$ over $[\mathbf{x}]$ by its tangent at the center $\bar{\mathbf{x}}$ of $[\mathbf{x}]$:

$$\mathbf{f}(\mathbf{x}) \simeq \mathbf{f}(\bar{\mathbf{x}}) + \mathbf{A} \cdot (\mathbf{x} - \bar{\mathbf{x}}) \tag{6}$$

The error of this approximation is

$$\mathbf{e}(\mathbf{x}) = \mathbf{f}(\bar{\mathbf{x}}) + \mathbf{A} \cdot (\mathbf{x} - \bar{\mathbf{x}}) - \mathbf{f}(\mathbf{x}) \tag{7}$$

An accurate box $[\mathbf{e}]([\mathbf{x}])$ containing $\mathbf{e}(\mathbf{x})$ on $[\mathbf{x}]$ can be obtained using the centered form [15]:

$$[\mathbf{e}]([\mathbf{x}]) = \mathbf{e}(\bar{\mathbf{x}}) + \frac{d\mathbf{e}}{d\mathbf{x}}([\mathbf{x}]) \cdot ([\mathbf{x}] - \bar{\mathbf{x}}) \tag{8}$$

or equivalently

$$[\mathbf{e}]([\mathbf{x}]) = \mathbf{e}(\bar{\mathbf{x}}) + \left(\mathbf{A} - \frac{d\mathbf{f}}{d\mathbf{x}}([\mathbf{x}])\right) \cdot ([\mathbf{x}] - \bar{\mathbf{x}}) \tag{9}$$

2.2 Polyhedron approximation of $\mathbb{X} \cap [\mathbf{x}]$

Proposition 1. *We have*

$$\left\{ \begin{array}{c} \mathbf{f}(\mathbf{x}) = \mathbf{0} \\ \mathbf{x} \in [\mathbf{x}] \end{array} \right. \Rightarrow \left\{ \begin{array}{c} \mathbf{A} \cdot \mathbf{x} \in [\mathbf{b}] \\ \mathbf{A} = \frac{d\mathbf{f}}{d\mathbf{x}}(\bar{\mathbf{x}}) \\ [\mathbf{b}] = \mathbf{A}\bar{\mathbf{x}} - \mathbf{f}(\bar{\mathbf{x}}) + [\mathbf{e}] \\ [\mathbf{e}] = \left(\mathbf{A} - \frac{d\mathbf{f}}{d\mathbf{x}}([\mathbf{x}])\right) \cdot ([\mathbf{x}] - \bar{\mathbf{x}}) \end{array} \right. \tag{10}$$

Proof. For $\mathbf{x} \in [\mathbf{x}]$, from (7) and (9), we have

$$\underbrace{\mathbf{f}(\bar{\mathbf{x}}) + \mathbf{A} \cdot (\mathbf{x} - \bar{\mathbf{x}}) - \mathbf{f}(\mathbf{x})}_{\mathbf{e}(\mathbf{x})} \in \underbrace{\left(\mathbf{A} - \frac{d\mathbf{f}}{d\mathbf{x}}([\mathbf{x}])\right) \cdot ([\mathbf{x}] - \bar{\mathbf{x}})}_{[\mathbf{e}]} \tag{11}$$

Since $\mathbf{f}(\mathbf{x}) = \mathbf{0}$, we get

$$\mathbf{f}(\bar{\mathbf{x}}) + \mathbf{A} \cdot (\mathbf{x} - \bar{\mathbf{x}}) \in [\mathbf{e}] \tag{12}$$

i.e.,

$$\mathbf{A} \cdot \mathbf{x} \in \underbrace{\mathbf{A}\bar{\mathbf{x}} - \mathbf{f}(\bar{\mathbf{x}}) + [\mathbf{e}]}_{[\mathbf{b}]} \tag{13}$$

□

As a consequence, the set $\mathbb{X} \cap [\mathbf{x}]$ is enclosed by the polyhedron defined as the intersection of the box $[\mathbf{x}]$ and the part of the space defined by $\mathbf{A} \cdot \mathbf{x} \in [\mathbf{b}]$. Now, polyhedrons are not easy to handle. For instance computing the projection of a polyhedron or even computing the interval hull is challenging as soon as we want guaranteed results. We prefer instead to use another type of wrapper which is easier to handle and which preserves the first order approximation, as introduced in the following section.

3 Gutters

A *gutter* a new type of abstract domain (or *wrapper*) (see [4] for more on abstract domains). Gutters will allow us to compute nonoverlapping paving of a solution set with a first order approximation. This is not possible to get these two features with classical wrappers such as boxes [15], ellipsoids[12], zonotopes [22][3] or octagons [14].

3.1 Notion of gutter

Definition 1. The *gutter* associated with a box $[\mathbf{x}] \subset \mathbb{R}^n$, a matrix $\mathbf{A}$, a vector $\mathbf{b}$ and the inflation rate ρ is the set $\langle \mathbf{x} \rangle$ defined by

$$\begin{array}{rcl} \langle \mathbf{x} \rangle & = & \langle [\mathbf{x}], \mathbf{A}, \mathbf{b}, \rho \rangle \\ & = & \{ \mathbf{x} \in [\mathbf{x}], \exists \mathbf{p}, \mathbf{A}\mathbf{p} = \mathbf{b} \text{ and } \|\mathbf{x} - \mathbf{p}\| < \rho \} . \end{array} \tag{14}$$

An illustration is given by Figure 3.

The quantity $\rho = \text{rad}(\langle \mathbf{x} \rangle)$ is called the *radius* of the gutter $\langle \mathbf{x} \rangle$. The affine space $\mathbf{A}\mathbf{p} = \mathbf{b}$ is called a *flat*.

Our motivation for using gutters is to have the following properties

- The box $[\mathbf{x}]$ in the structure of the gutter will allow us to build a nonoverlapping covering of $\mathbb{X}$. This is not the case for zonotopes.
- A gutter can easily be bisected, contrary to ellipsoids.
- The axis-aligned projection is easy with gutters, contrary to polyhedrons.

- A first order approximation is possible, contrary to boxes.

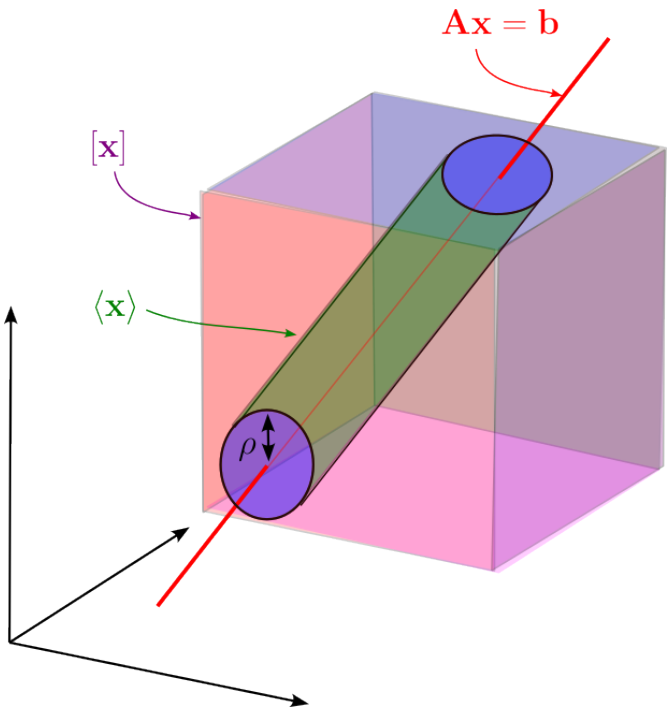

Figure 3: The gutter (green) is here the intersection between the box $[\mathbf{x}]$ and a cylinder

3.2 Axis aligned projection of a gutter

Consider the gutter (see (14)) $\langle \mathbf{x} \rangle = \langle [\mathbf{x}], \mathbf{A}, \mathbf{b}, \rho \rangle$. The vector $\mathbf{x} = (\mathbf{x}_1, \mathbf{x}_2) \in \mathbb{R}^n$, with $\mathbf{x}_1 \in \mathbb{R}^m$ and $\mathbf{x}_2 \in \mathbb{R}^{n-m}$.

Definition 2. We define the orthogonal projection of the gutter $\langle \mathbf{x} \rangle = \langle [\mathbf{x}], \mathbf{A}, \mathbf{b}, \rho \rangle$ in the $\mathbf{x}_1$-space as follows

$$\text{proj}_{1:m}(\langle [\mathbf{x}], \mathbf{A}, \mathbf{b}, \rho \rangle) =< [\mathbf{x}_1], \mathbf{A}^{\text{proj}}, \mathbf{b}^{\text{proj}}, \rho > \tag{15}$$

where

$$\begin{array}{rcl} (\mathbf{A}_1, \mathbf{A}_2) & = & \mathbf{A} \\ \mathbf{A}^{\text{proj}} & = & \left(\mathbf{A}_1^{-1}\mathbf{A}_2\right)^{\perp} \\ \mathbf{b}^{\text{proj}} & = & \mathbf{A}^{\text{proj}}\mathbf{A}_1^{-1}\mathbf{b} \\ [\mathbf{x}_1] & = & \text{proj}_{1:m}([\mathbf{x}]) \end{array} \tag{16}$$

In this definition, $\text{proj}_{1:m}$ denotes the orthogonal projection with respect to the first m entries. Figure 4 illustrates the projection in the case where $m = 2$ and $n = 3$.

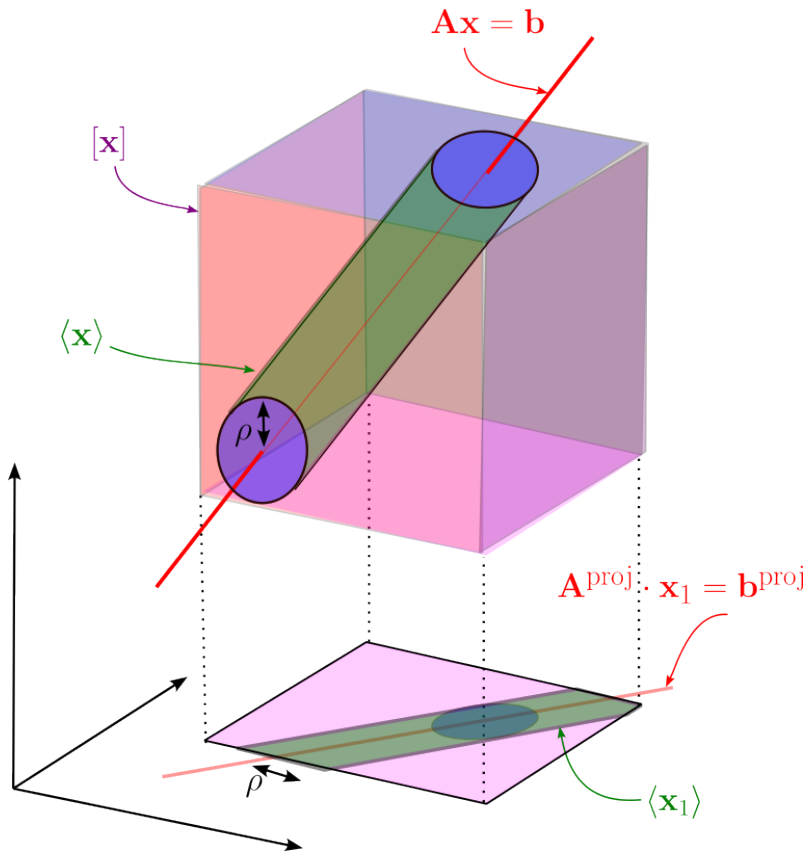

Figure 4: Projection of $\langle \mathbf{x} \rangle$ on the horizontal plane

Proposition 2. *If* $\mathbf{x} \in \langle [\mathbf{x}], \mathbf{A}, \mathbf{b}, \rho \rangle$*, then* $proj_{1:m}\mathbf{x} \in proj_{1:m}(\langle [\mathbf{x}], \mathbf{A}, \mathbf{b}, \rho \rangle)$*. See Definition 2 for the projection of a gutter.*

Proof. We have to prove that if $\mathbf{x} \in \langle [\mathbf{x}], \mathbf{A}, \mathbf{b}, \rho \rangle$, then, $\mathbf{x}_1 = \text{proj}_{1:m}\mathbf{x} = \left\langle [\mathbf{x}_1], \mathbf{A}^{\text{proj}}, \mathbf{b}^{\text{proj}}, \rho \right\rangle$.

(i) The fact that $\mathbf{x}_1 \in [\mathbf{x}_1] \in \text{proj}_{1:m}([\mathbf{x}])$ is trivial.

(ii) Take $\mathbf{x} = (\mathbf{x}_1, \mathbf{x}_2)$ such that $\mathbf{Ax} = \mathbf{b}$. We now check that is projection $\mathbf{x}_1$ satisfies

$$\mathbf{A}^{\text{proj}} \cdot \mathbf{x}_1 = \mathbf{b}^{\text{proj}}. \tag{17}$$

We have

$$\mathbf{A}_1\mathbf{x}_1 + \mathbf{A}_2\mathbf{x}_2 = \mathbf{b} \tag{18}$$

i.e.,

$$\mathbf{x}_1 = \mathbf{A}_1^{-1}\mathbf{b} - \mathbf{A}_1^{-1}\mathbf{A}_2\mathbf{x}_2 \tag{19}$$

or equivalently,

$$\underbrace{\mathbf{x}_1 - \mathbf{A}_1^{-1}\mathbf{b}}_{\mathbf{y}} = \underbrace{-\mathbf{A}_1^{-1}\mathbf{A}_2}_{\mathbf{M}} \cdot \underbrace{\mathbf{x}_2}_{\mathbf{b}}. \tag{20}$$

Now, recall that

$$\mathbf{y} = \mathbf{M} \cdot \mathbf{b} \Leftrightarrow \mathbf{N}\mathbf{y} = \mathbf{0} \tag{21}$$

where $\mathbf{N}$ is orthogonal to $\mathbf{M}$, denoted by $\mathbf{N} = \mathbf{M}^{\perp}$. Indeed, if $\mathbf{y}$ is a linear combination of the columns of $\mathbf{M}$ (*i.e.*, $\mathbf{y} = \mathbf{M} \cdot \mathbf{b}$). It means that $\mathbf{y}$ is orthogonal to the null space of $\mathbf{M}$ (*i.e.*, $\mathbf{N}\mathbf{y} = \mathbf{0}$). As a consequence

$$-\left(\mathbf{A}_1^{-1}\mathbf{A}_2\right)^{\perp}\left(\mathbf{x}_1 - \mathbf{A}_1^{-1}\mathbf{b}\right) = \mathbf{0} \tag{22}$$

i.e.,

$$\underbrace{\left(\mathbf{A}_1^{-1}\mathbf{A}_2\right)^{\perp}}_{\mathbf{A}^{\text{proj}}} \cdot \mathbf{x}_1 = \underbrace{\left(\mathbf{A}_1^{-1}\mathbf{A}_2\right)^{\perp}\mathbf{A}_1^{-1}\mathbf{b}}_{\mathbf{b}^{\text{proj}}}. \tag{23}$$

(iii) Take now $\mathbf{x} = (\mathbf{x}_1, \mathbf{x}_2)$ such that $\mathbf{x}$ is at a distance to the flat $\mathbb{P} : \mathbf{A}\mathbf{x} = \mathbf{b}$ less that ρ. Then $\mathbf{x}_1$ is at a distance to $\text{proj}_{1:m}\mathbb{P}$, less that ρ. This is due to the property that any orthogonal projection is non-expansive, meaning they do not increase distances. □

The corresponding Python code compute the projection of a gutter.

```
def project_gutter_x1x2(A,b):
   m,n=A.shape[0],A.shape[1]
   A1=A[:,0:m]
   A2=A[:,m:n]
   U,S,Vt = np.linalg.svd((inv(A1)@A2).T)
   Aproj= (Vt.T[:,n-m:]).T
   return Aproj, Aproj@inv(A1)@b
```

Illustration

To explain the procedure, take $m = 2$ and $n = 3$. The system becomes.

$$\underbrace{\begin{pmatrix} a_{11} & a_{12} & a_{13} \\ a_{21} & a_{22} & a_{23} \end{pmatrix}}_{\mathbf{A}} \begin{pmatrix} x_1 \\ x_2 \\ x_3 \end{pmatrix} = \underbrace{\begin{pmatrix} b_1 \\ b_2 \end{pmatrix}}_{\mathbf{b}} \tag{24}$$

After the elimination of x_3 we get

$$(a_{23}a_{11} - a_{13}a_{21})\, x_1 + (a_{23}a_{12} - a_{13}a_{22})\, x_2 \;=\; a_{23}b_1 - a_{13}b_2 \tag{25}$$

Therefore, we can write

$$\mathrm{proj}_{1:2}(\langle [\mathbf{x}], \mathbf{A}, \mathbf{b}, \rho \rangle) = \left\langle [\mathbf{x}_1], \mathbf{A}^{\mathrm{proj}}, b^{\mathrm{proj}}, \rho \right\rangle \tag{26}$$

where

$$\begin{array}{rcc} \mathbf{A}^{\mathrm{proj}} & = & \begin{pmatrix} a_{23}a_{11} - a_{13}a_{21} & a_{23}a_{12} - a_{13}a_{22} \end{pmatrix} \\ b^{\mathrm{proj}} & = & a_{23}b_1 - a_{13}b_2 \end{array} \tag{27}$$

3.3 Intersection between two gutters

Definition 3. We define the intersection between the gutter $\langle \mathbf{x}_1 \rangle = \langle [\mathbf{x}]_1, \mathbf{A}_1, \mathbf{b}_1, \rho_1 \rangle$ and the gutter $\langle \mathbf{x}_2 \rangle = \langle [\mathbf{x}]_2, \mathbf{A}_2, \mathbf{b}_2, \rho_2 \rangle$ as

$$\langle \mathbf{x}_1 \rangle \cap \langle \mathbf{x}_2 \rangle = \langle [\mathbf{x}]_3, \mathbf{A}_3, \mathbf{b}_3, \rho_3 \rangle \tag{28}$$

where

$$\begin{array}{rcc} [\mathbf{x}]_3 & = & [\mathbf{x}]_1 \cap [\mathbf{x}]_2 \\ \mathbf{A}_3 & = & \begin{pmatrix} \mathbf{A}_1 \\ \mathbf{A}_2 \end{pmatrix} \\ \mathbf{b}_3 & = & \begin{pmatrix} \mathbf{b}_1 \\ \mathbf{b}_2 \end{pmatrix} \\ \rho_3 & = & \frac{1}{\sin\theta}\sqrt{\rho_b^2 + \rho_a^2 + 2\rho_a\rho_b \cdot \cos\theta} \end{array} \tag{29}$$

where θ is the principle angle between the two spaces generated by $\mathbf{A}_1$ and $\mathbf{A}_2$.

Figure 5 illustrates the projection in the case where $m = 2$ and $n = 3$. To compute θ, we first compute the null space matrices $\mathbf{K}_1, \mathbf{K}_2$ for $\mathbf{A}_1, \mathbf{A}_2$. Then we get

$$\theta = \arcsin \sqrt{1 - \sigma_{\max}^2(\mathbf{K}_1^{\mathrm{T}} \mathbf{K}_2)} \tag{30}$$

where $\sigma_{\max}$ returns the largest singular value.

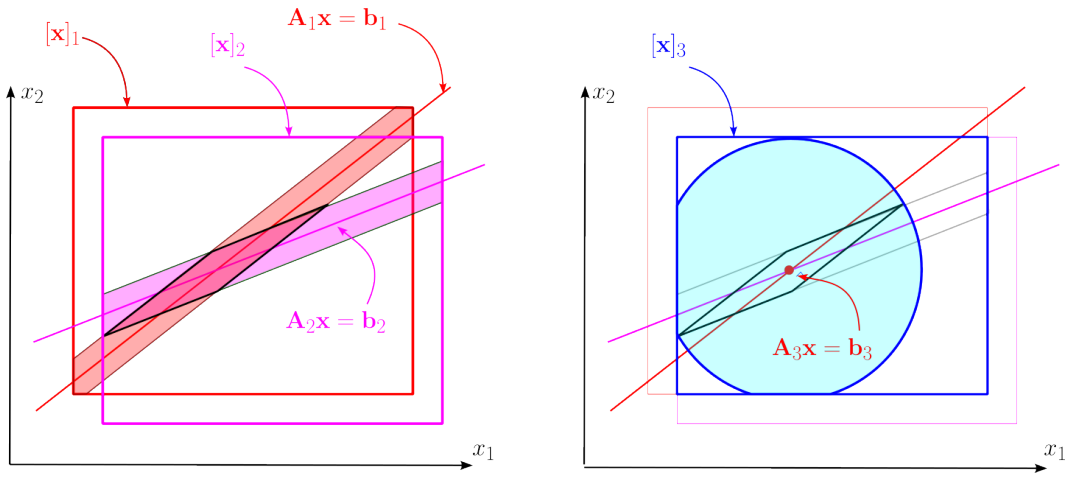

Figure 5: The blue set on the right corresponds the gutter intersection between the two gutters on the left

Proposition 3. *If* $\mathbf{x} \in \langle \mathbf{x}_1 \rangle$ *and* $\mathbf{x} \in \langle \mathbf{x}_2 \rangle$ *then* $\mathbf{x} \in \langle \mathbf{x}_1 \rangle \cap \langle \mathbf{x}_2 \rangle$.

Proof. The nontrivial point is the radius ρ_3. From the construction of Figure 6, we have

$$\begin{aligned} b \sin\theta &= h_a \\ a \sin\theta &= h_b \end{aligned}$$

Moreover, from the law of cosines, the diameter of the parallelogram is

$$\begin{aligned} d &= \sqrt{a^2 + b^2 + 2ab \cdot |\cos\theta|} \\ &= \sqrt{\tfrac{h_b^2}{\sin^2\theta} + \tfrac{h_a^2}{\sin^2\theta} + 2\tfrac{h_a h_b}{\sin^2\theta} \cdot |\cos\theta|} \\ &= \tfrac{1}{|\sin\theta|} \sqrt{h_b^2 + h_a^2 + 2h_a h_b \cdot |\cos\theta|} \end{aligned} \tag{31}$$

We conclude that

$$\rho_3 = \frac{1}{\sin\theta} \sqrt{\rho_b^2 + \rho_a^2 + 2\rho_a \rho_b \cdot \cos\theta} \tag{32}$$

□

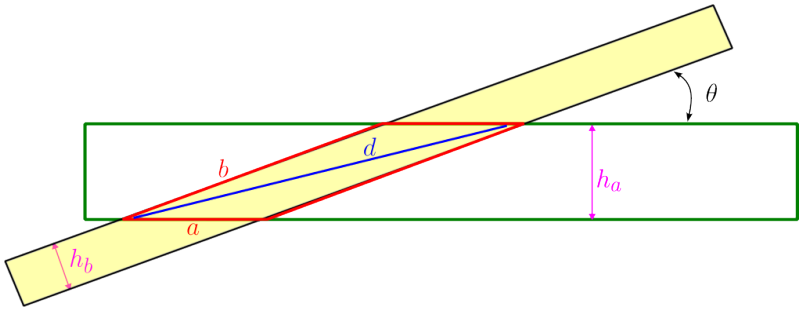

Figure 6: Computation of the diameter of the parallelogram

4 Gutter contractors

We consider again the set

$$\mathbb{X} = \{\mathbf{x} \in [\mathbf{x}] | \mathbf{f}(\mathbf{x}) = \mathbf{0}\} \tag{33}$$

where $\mathbf{f}(\mathbf{x}) \in \mathbb{R}^m$ and $\mathbf{x} \in \mathbb{R}^n$, $m < n$. We take a box $[\mathbf{x}]$. We want to compute a gutter $\langle \mathbf{x} \rangle = \langle [\mathbf{x}], \mathbf{A}, \mathbf{b}, \rho \rangle$ enclosing $\mathbb{X} \cap [\mathbf{x}]$. The radius $\rho = \text{rad}(\langle \mathbf{x} \rangle)$ represents the inflation to be done for the flat $\mathbf{Ax} = \mathbf{b}$ to enclose $\mathbb{X} \cap [\mathbf{x}]$. Equivalently, ρ corresponds to the Hausdorff distance $h(\langle \mathbf{x} \rangle, \mathbb{X} \cap [\mathbf{x}])$ between $\mathbb{X} \cap [\mathbf{x}]$ and $\langle \mathbf{x} \rangle$.

Proposition 4. *Consider the subspace of* $\mathbb{R}^n$

$$\mathbb{E}_0 = \{\mathbf{x} \in \mathbb{R}^n \mid \mathbf{Ax} = \mathbf{0}\}. \tag{34}$$

The orthogonal projection of a vector $\mathbf{y}$ *on* $\mathbb{E}_0$ *is given by*

$$\hat{\mathbf{y}} = \left(\mathbf{I} - \mathbf{A}^T \left(\mathbf{A}\mathbf{A}^T\right)^{-1} \mathbf{A}\right) \mathbf{y}. \tag{35}$$

Proof. Denote by $\mathbf{a}_i$ the vector corresponding to the ith row of $\mathbf{A}$, *i.e.*,

$$\mathbf{A}^{\mathrm{T}} = (\mathbf{a}_1 | \dots | \mathbf{a}_m). \tag{36}$$

The set $\mathbb{E}_0$ corresponds to the set of all $\mathbf{x}$ that are orthogonal to all $\mathbf{a}_j$. Equivalently, the vector space $\mathbb{A} = \text{span}(\mathbf{a}_1, \mathbf{a}_2, \dots)$ generated by the $\mathbf{a}_i$, satisfies

$$\mathbb{A} = \mathbb{E}_0^{\perp} \tag{37}$$

and

$$\mathbb{E}_0 = \mathbb{A}^{\perp}. \tag{38}$$

Denote by $\tilde{\mathbf{y}}$ the orthogonal projection of $\mathbf{y}$ on $\mathbb{A}$.

$$\tilde{\mathbf{y}} = \tilde{p}_1\mathbf{a}_1 + \cdots + \tilde{p}_m\mathbf{a}_m = \mathbf{A}^{\mathrm{T}}\tilde{\mathbf{p}} \tag{39}$$

where

$$\tilde{\mathbf{p}} = (\tilde{p}_1, \ldots, \tilde{p}_m)^{\mathrm{T}} = \operatorname{argmin}\left\{\|\mathbf{y} - \mathbf{A}^{\mathrm{T}}\tilde{\mathbf{p}}\|, \mathbf{p} \in \mathbb{R}^m\right\}. \tag{40}$$

Using the least-square formula, we get that

$$\tilde{\mathbf{p}} = \left(\mathbf{A}\mathbf{A}^{\mathrm{T}}\right)^{-1}\mathbf{A}\mathbf{y}, \tag{41}$$

i.e.,

$$\tilde{\mathbf{y}} = \mathbf{A}^{\mathrm{T}}\left(\left(\mathbf{A}\mathbf{A}^{\mathrm{T}}\right)^{-1}\mathbf{A}\mathbf{y}\right) \tag{42}$$

Now, as illustrated by Figure 7, we have $\hat{\mathbf{y}} = \mathbf{y} - \tilde{\mathbf{y}}$. Thus

$$\hat{\mathbf{y}} = \mathbf{y} - \tilde{\mathbf{y}} = \left(\mathbf{I} - \mathbf{A}^{\mathrm{T}}\left(\mathbf{A}\mathbf{A}^{\mathrm{T}}\right)^{-1}\mathbf{A}\right)\mathbf{y}. \tag{43}$$

□

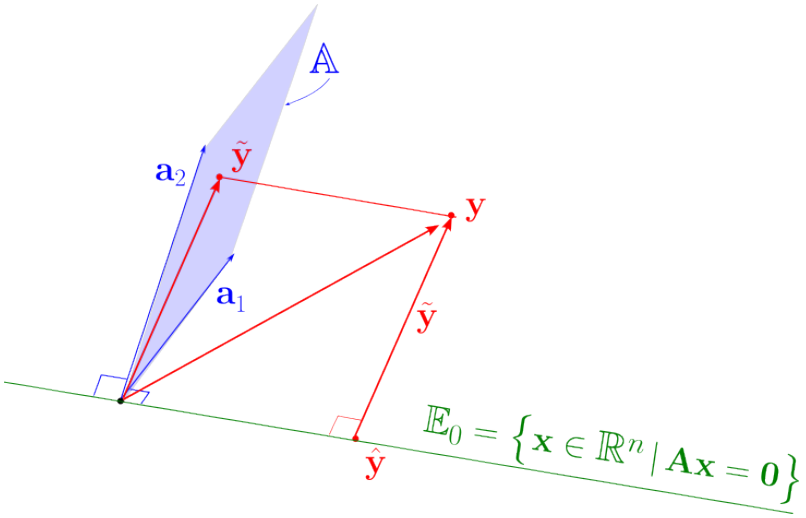

Figure 7: Projection of $\mathbf{y}$ on $\mathbb{E}_0$

Proposition 5. *Consider the two flats of* $\mathbb{R}^n$

$$\begin{aligned} \mathbb{E}_1 &= \{\mathbf{x} \in \mathbb{R}^n \,|\, \mathbf{A}\mathbf{x} = \mathbf{b}_1\} \\ \mathbb{E}_2 &= \{\mathbf{x} \in \mathbb{R}^n \,|\, \mathbf{A}\mathbf{x} = \mathbf{b}_2\} \end{aligned} \tag{44}$$

The Hausdorff distance [2] between $\mathbb{E}_1$ *and* $\mathbb{E}_2$ *is*

$$h(\mathbb{E}_1, \mathbb{E}_2) = \|\mathbf{A}^T\left(\mathbf{A}\mathbf{A}^T\right)^{-1}(\mathbf{b}_1 - \mathbf{b}_2)\| \tag{45}$$

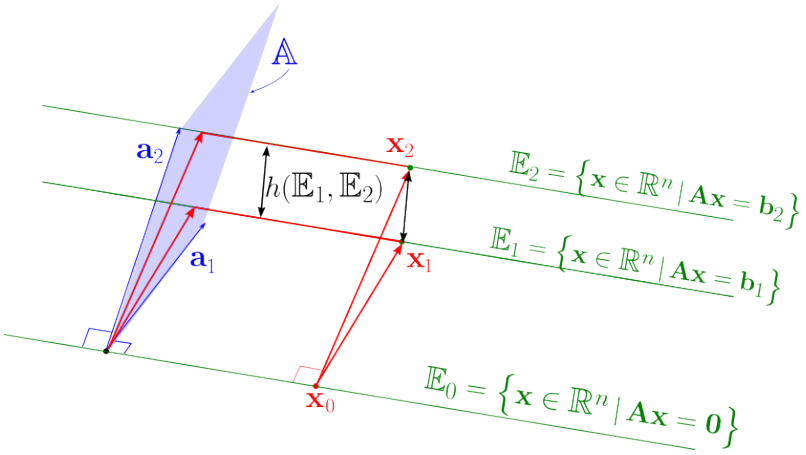

Figure 8: Hausdorff distance between $\mathbb{E}_1$ and $\mathbb{E}_2$

The proposition is illustrated by Figure 8.

Proof. First note that both $\mathbb{E}_1$, $\mathbb{E}_2$ and $\mathbb{E}_0 = \{\mathbf{x} \in \mathbb{R}^n \,|\, \mathbf{A}\mathbf{x} = \mathbf{0}\}$ are all orthogonal to $\mathbb{A}$. Take one point $\mathbf{x}_1 \in \mathbb{E}_1$. The nearest $\mathbf{x}_2 \in \mathbb{E}_2$ to $\mathbf{x}_1$ is such that the orthogonal projection of $\mathbf{x}_1$ and $\mathbf{x}_2$ on $\mathbb{E}_0$ corresponds to the same point $\mathbf{x}_0$. Equivalently

$$\mathbf{x}_0 = \left(\mathbf{I} - \mathbf{A}^{\mathrm{T}} \left(\mathbf{A}\mathbf{A}^{\mathrm{T}}\right)^{-1} \mathbf{A}\right) \mathbf{x}_1 = \left(\mathbf{I} - \mathbf{A}^{\mathrm{T}} \left(\mathbf{A}\mathbf{A}^{\mathrm{T}}\right)^{-1} \mathbf{A}\right) \mathbf{x}_2. \tag{46}$$

Therefore

$$\mathbf{x}_1 - \mathbf{x}_2 = \mathbf{A}^{\mathrm{T}} \left(\mathbf{A}\mathbf{A}^{\mathrm{T}}\right)^{-1} \mathbf{A} \left(\mathbf{x}_1 - \mathbf{x}_2\right) \tag{47}$$

i.e.,

$$\mathbf{x}_1 - \mathbf{x}_2 = \mathbf{A}^{\mathrm{T}} \left(\mathbf{A}\mathbf{A}^{\mathrm{T}}\right)^{-1} \left(\mathbf{b}_1 - \mathbf{b}_2\right). \tag{48}$$

□

The following proposition tells us how to build a gutter enclosing $\mathbb{X} \cap [\mathbf{x}]$.

Definition 4. Consider a set $\mathbb{X}$ of $\mathbb{R}^n$. A *gutter contractor* $\mathcal{B}$ associated to $\mathbb{X}$ is an operator which takes as input a box $[\mathbf{x}]$ and returns a gutter $\langle [\mathbf{x}], \mathbf{A}, \mathbf{b}, \rho \rangle$ such that

$$\mathbb{X} \cap [\mathbf{x}] \;\subset\; \langle [\mathbf{x}], \mathbf{A}, \mathbf{b}, \rho \rangle \,. \tag{49}$$

Moreover, $\mathcal{B}$ is said to have an order k if for all nested sequence of boxes converging to a point $\mathbf{x}$ in $\mathbb{X}$,

$$\frac{h(\langle [\mathbf{x}], \mathbf{A}, \mathbf{b}, \rho \rangle, \mathbb{X} \cap [\mathbf{x}])}{\mathrm{rad}([\mathbf{x}])^k} \to 0. \tag{50}$$

where rad([**x**]) is the radius of the box [**x**].

Proposition 6. *Consider the set* $\mathbb{X} = \{\mathbf{x} \in \mathbb{R}^n | \mathbf{f}(\mathbf{x}) = \mathbf{0}\}$. *The operator*

$$\mathcal{B} : [\mathbf{x}] \rightarrow \langle [\mathbf{x}], \mathbf{A}, \mathbf{b}, \rho \rangle \tag{51}$$

where

$$\begin{array}{rcl} \mathbf{b} & = & \mathbf{A}\bar{\mathbf{x}} - \mathbf{f}(\bar{\mathbf{x}}) \\ \mathbf{A} & = & \frac{\partial \mathbf{f}}{\partial \mathbf{x}}(\bar{\mathbf{x}}) \\ \rho & = & \sigma_{\mathbf{A}} \cdot ub\|[\mathbf{e}]\| \\ [\mathbf{e}] & = & \left(\mathbf{A} - \frac{d\mathbf{f}}{d\mathbf{x}}([\mathbf{x}])\right) \cdot ([\mathbf{x}] - \bar{\mathbf{x}}) \end{array} \tag{52}$$

and where $\sigma_{\mathbf{A}} = \|\mathbf{A}^T \left(\mathbf{A}\mathbf{A}^T\right)^{-1}\|_2$ *is the spectral norm of the matrix* $\mathbf{A}^T \left(\mathbf{A}\mathbf{A}^T\right)^{-1}$ *is a gutter contractor of order 1.*

Proof. From Proposition 1, we know that

$$\left\{ \begin{array}{c} \mathbf{f}(\mathbf{x}) = \mathbf{0} \\ \mathbf{x} \in [\mathbf{x}] \end{array} \right. \Rightarrow \left\{ \begin{array}{c} \mathbf{A} \cdot \mathbf{x} = \tilde{\mathbf{b}} \\ \tilde{\mathbf{b}} = \mathbf{A}\bar{\mathbf{x}} - \mathbf{f}(\bar{\mathbf{x}}) + \mathbf{e} \\ \mathbf{e} \in [\mathbf{e}] \end{array} \right. \tag{53}$$

Take $\mathbb{E} : \mathbf{A} \cdot \mathbf{x} = \mathbf{b}$ and $\tilde{\mathbb{E}} : \mathbf{A} \cdot \mathbf{x} = \tilde{\mathbf{b}}$. From Proposition 5,

$$h(\mathbb{E}, \tilde{\mathbb{E}}) = \|\mathbf{A}^{\mathrm{T}} \left(\mathbf{A}\mathbf{A}^{\mathrm{T}}\right)^{-1} \left(\mathbf{b} - \tilde{\mathbf{b}}\right)\| \leq \sigma_{\mathbf{A}} \cdot \|\mathbf{b} - \tilde{\mathbf{b}}\| \tag{54}$$

It means that

$$\begin{array}{c} \exists \mathbf{p} \in \mathbb{R}^n, \mathbf{A} \cdot \mathbf{p} = \mathbf{b} \\ \|\mathbf{p} - \mathbf{x}\| \leq \sigma_{\mathbf{A}} \cdot \|\mathbf{e}\| \end{array} \tag{55}$$

The order 1 for the gutter contractor comes from the fact that

$$\frac{\mathrm{rad}\left(\left(\mathbf{A} - \frac{d\mathbf{f}}{d\mathbf{x}}([\mathbf{x}])\right) \cdot ([\mathbf{x}] - \bar{\mathbf{x}})\right)}{\mathrm{rad}([\mathbf{x}])} \rightarrow 0 \tag{56}$$

which is a property of the centered form [15]. □

5 Test-cases

We consider here three testcases from the literature. For each of these test-case, we have to solve a system of 3 variables with two nonlinear equations

$$\begin{array}{rcl} f_1(x_1, x_2, x_3) & = & 0 \\ f_2(x_1, x_2, x_3) & = & 0 \end{array} \tag{57}$$

We want to characterize the set

$$\mathbb{X} = \{(x_1, x_2, x_3) \,|\, \mathbf{f}(x_1, x_2, x_3) = \mathbf{0}\}\,. \tag{58}$$

In the following, the solutions will be depicted on the (x_1, x_2)- space.

5.1 Algorithm

For the resolution, we use a branch and prune algorithm such as SIVIA (see *e.g.* [10]). Now, we take advantage of the gutter contractor $\mathcal{B}$ for the solution set $\mathbb{X} \in \mathbb{R}^3$. A paving with boxes is generated and the current paving is stored in a list $\mathcal{L}$. The final gutters are stored in $\mathbb{X}^+$. The algorithm can be described as follows.

Initialization: $\mathcal{L} = \{[\mathbf{x}]\}$; $\mathbb{X}^+ = \{\}$.

Resolution.

- **Contraction step**. Replace each $[\mathbf{x}] \in \mathcal{L}$, by the smallest box enclosing the gutter $\langle\mathbf{x}\rangle = \mathcal{B}([\mathbf{x}])$.
- **Bisection step**. For each $[\mathbf{x}] \in \mathcal{L}$, if $[\mathbf{x}]$ is too small then push $\langle\mathbf{x}\rangle$ on $\mathbb{X}^+$, otherwise, bisect $[\mathbf{x}]$ and push the two resulting boxes in $\mathcal{L}$.

By too small, we mean

$$\text{rad}([\mathbf{x}]) < \varepsilon \text{ or } \text{rad}(\langle\mathbf{x}\rangle) < 0.01\varepsilon \tag{59}$$

where ε is a small positive number corresponding the desired accuracy. The condition $\text{rad}([\mathbf{x}]) < \varepsilon$ is classical in many interval based algorithm. The condition $\text{rad}(\langle\mathbf{x}\rangle) < 0.01\varepsilon$ tells us that if we have a large box $[\mathbf{x}]$ such that its gutter approximation is already much more precise than what we want, then there is no need to bisect it. This condition may reduce drastically the number of generated boxes.

Moreover, in the definition of the solution set $\mathbb{P}$ (see (58)), we only want to enclose the projection of $\mathbb{X} \subset \mathbb{R}^3$. Each gutter of $\langle\mathbf{x}\rangle$ of $\mathbb{X}^+$ should thus be projected on the (x_1, x_2) space, as explained in Subsection3.2.

5.2 Delay system

Consider the linear time-delay system [21] given by

$$\ddot{y} + 2\dot{y}(t - x_1) + y(t - x_2) = 0 \tag{60}$$

where x_1, x_2 are two parameters. Its characteristic function is

$$\theta(\mathbf{x}, s) = s^2 + 2se^{-sx_1} + e^{-sx_2}. \tag{61}$$

The location of the roots for $\theta(x_1, x_2, jx_3)$, where $j^2 = -1$, provides a good understanding of the stability of the system. As in [21], we define the set

$$\{(x_1, x_2) \,|\, \exists x_3 \in [0, 10],\, \theta(\mathbf{p}, jx_3) = 0\}. \tag{62}$$

Since

$$\begin{array}{ll} & \theta(x_1, x_2, jx_3) = 0 \\ \Leftrightarrow & \mathbf{f}(\mathbf{x}) = \begin{pmatrix} -x_3^2 + 2x_3 \sin(x_3 x_1) + \cos(x_3 x_2) \\ 2x_3 \cos(x_3 x_1) - \sin(x_3 x_2) \end{pmatrix} = \mathbf{0} \end{array} \tag{63}$$

the resolution can be done using our algorithm. Different cases have been treated, as illustrated by the following table. In Figure 9 the lines correspond to different cases (a,b,c,d). The left column shows the paving obtained using one of the best (to my knowledge) interval method with a contractor which is asymptotically minimal [8]. The right column shows the paving obtained by gutter contractors. Several initial boxes have been taken with different accuracy ε. The computing time is denoted by T_1 for the interval contractor and T_2 for the gutter contractor. The volume of the approximation is denoted by V_1 for the interval contractor and V_2 for the gutter contractor. We observe that the improvement becomes significant when ε is small. Indeed, the approximation is more accurate and the computing time is lower. It is a consequence of the first order approximation of the gutter contractor.

	Case (a)	Case (b)	Case (c)	Case (d)
$[\mathbf{x}]$	$\begin{pmatrix} [0,2] \\ [2,4] \\ [0,10] \end{pmatrix}$	$\begin{pmatrix} [1.3,1.8] \\ [3,3.5] \\ [0,10] \end{pmatrix}$	$\begin{pmatrix} [1.595,1.615] \\ [3.2,3.22] \\ [0,10] \end{pmatrix}$	$\begin{pmatrix} [1.601,1.603] \\ [3.202,3.206] \\ [0,10] \end{pmatrix}$
ε	2^{-4}	2^{-8}	2^{-12}	2^{-16}
$T_1(s)$	0.51	0.84	0.11	0.19
$T_2(s)$	0.86	1.46	0.17	0.05
V_1	0.092	$2.05 \cdot 10^{-3}$	$3.06 \cdot 10^{-6}$	$4.18 \cdot 10^{-7}$
V_2	0.02	$1.93 \cdot 10^{-3}$	$7.2 \cdot 10^{-7}$	$5.78 \cdot 10^{-9}$
$\frac{V_1}{V_2}$	3.8	4.6	15.3	72.4

For Case (a), we observe that the gutters do not yield any improvement. When ε decreases, we become more and more accurate with respect to an interval approximation (represented by the ratio V_1/V_2) and the resulting computing time is reduced. In subfigure (a), right, we observe many red boxes. For these boxes, we were unable to get any gutter contraction on only the interval contractor has been needed. In Subfigure (c), right, the blue boxes on the right are large compared to the left boxes. This is due to the fact that the for the right boxes, the gutter approximation is good enough to be stored in $\mathbb{X}^+$ without any further bisection. In Subfigure (d) right, all blue boxes are such that $\text{rad}(\mathcal{B}([\mathbf{x}])) < 0.01\varepsilon$. The stop criterion $\text{rad}([\mathbf{x}]) < \varepsilon$ is not needed anymore. Compared to the classical approach (see Subfigure (d) left), many boxes have to be generated to reach the condition $\text{rad}([\mathbf{x}]) < \varepsilon$. This explains why gutters become much more efficient as soon as a high accuracy is required.

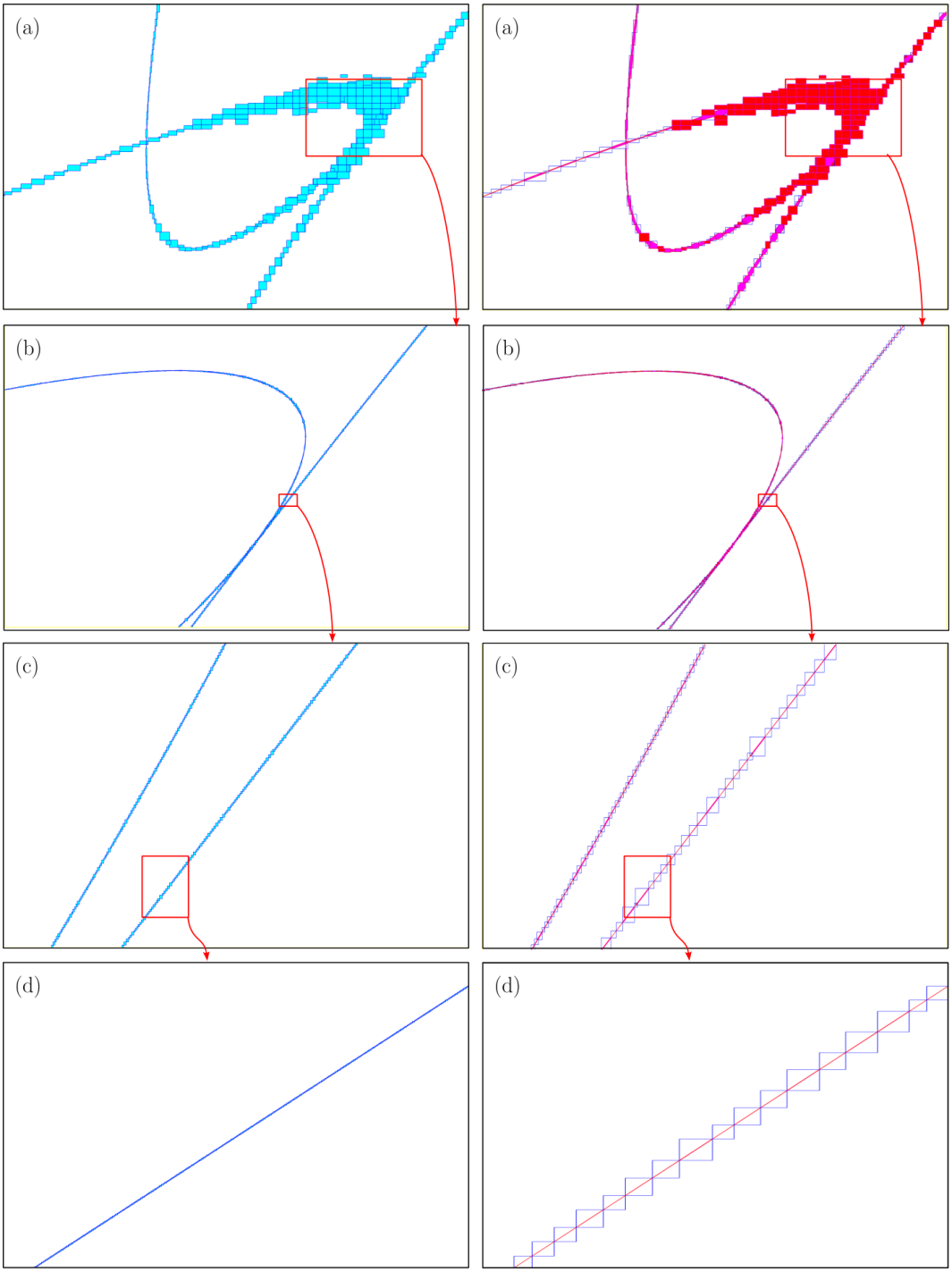

Figure 9: Left: resolution with asymptotically minimal contractors; Right: resolution with gutter contractors

5.3 Tensegrity

Consider robot described by Figure 10 with three springs (green) and three rigid bars (see [1], pps. 182–183 for more details). The length x_1 of the red rigid bar can be tuned. The magenta bar can slide with no friction along the blue bar.

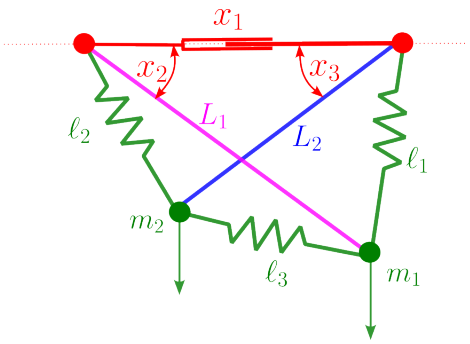

Figure 10: Tensegrity system, only x_1 can be controlled

At the equilibrium, the potential energy U of the mechanism, given by:

$$\begin{array}{rcl} U & = & \frac{k}{2}\left(\ell_1^2+\ell_2^2+\ell_3^2\right) - m_1 L_1 \sin x_2 - m_2 L_2 \sin x_3 \\ & = & \frac{k}{2}\left(3x_1^2 - 4L_1 x_1 \cos\theta_1 + 2\left(L_1^2+L_2^2+L_1 L_2\cos(x_2+x_3) - 4L_2 x_1 \cos x_3\right)\right) \\ & & -m_1 L_1 \sin x_2 - m_2 L_2 \sin x_3 \end{array} \tag{64}$$

should be stationary [23], *i.e.*,

$$\begin{array}{rcl} \frac{\partial U}{\partial \theta_1} & = & 0 \\ \frac{\partial U}{\partial \theta_2} & = & 0 \end{array} \tag{65}$$

We get

$$\begin{array}{rcl} kL_1\sin(x_2+x_3) - 2kx_1\sin x_3 + m_2\cos x_3 & = & 0 \\ kL_2\sin(x_2+x_3) - 2kx_1\sin x_2 + m_1\cos x_2 & = & 0 \end{array} \tag{66}$$

As in [23], we want to characterize the set of all $(x_1, x_2) \in [0,2]\times[-\pi,\pi]$ such that there exists $x_3 \in [-\pi,\pi]$ for which the two equations are satisfied. For $\varepsilon = 2^{-8}$, $L_1 = 1$, $k = 100$, $m_1 = m_2 = 5$, and $L_2 \in \{0.99, 1, 1.05\}$, our algorithm generates Figure 11 (bottom), to be compared with the symbolic approach of [23]. For our algorithm, the computing time is less than 1sec. No computing time is given in [23].

In the workspace, a discrete approximation of the occupancy set is depicted on Figure 12.

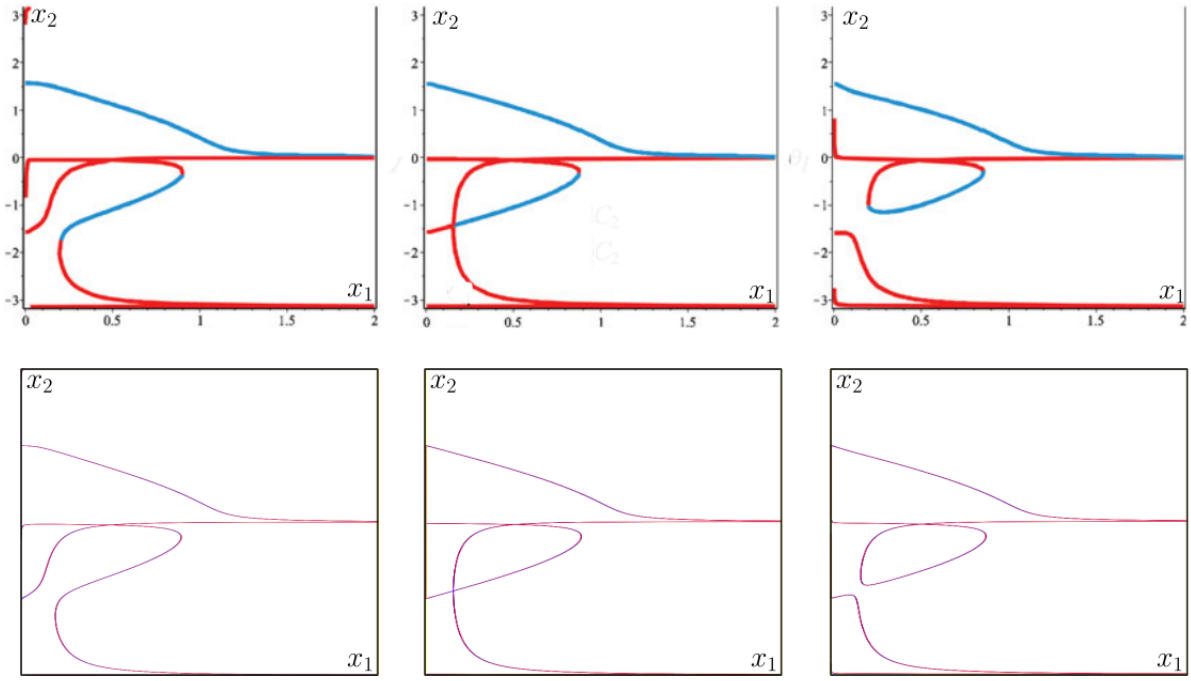

Figure 11: Set of all (x_1, x_2) corresponding to an equilibrium; Top: symbolic approach by Wenger and Chablat; Bottom: with gutters
Left: $L_2 = 0.99$, Center: $L_2 = 1$; Right: $L_2 = 1.05$

5.4 RP-5AH robot

We consider the example taken from [13] with the robot RP-5AH made by Mitsubishi, as illustrated by Figure 13. The parameters are taken as $a_1 = -1$, $a_2 = 0$, $b_1 = 1$, $b_2 = 0$, $\ell_1 = \ell_2 = \frac{3}{2}$, $\ell_3 = \ell_4 = 2$. For this robot, we can control the two angles x_1 and x_2 that are linked by the constraint that the point $\mathbf{p}$ should belong to the Lissajou curve of equation

$$\mathbf{p}(x_3) = \begin{pmatrix} \sin x_3 \\ \frac{3}{2} + \cos(3x_3) \end{pmatrix} \tag{67}$$

for some $x_3 \in [0, 2\pi]$. Equivalently [13], we want to characterize the set of all (x_1, x_2) such that there exists $x_3 \in [0, 2\pi]$ such that

$$\begin{array}{rcl} (\sin x_3 - \ell_3 \cos x_1 - a_1)^2 + (\frac{3}{2} + \cos(3x_3) - \ell_3 \sin x_1 + a_2)^2 - \ell_1^2 & = & 0 \\ (\sin x_3 - \ell_4 \cos x_2 - b_1)^2 + (\frac{3}{2} + \cos(3x_3) - \ell_4 \sin x_2 - b_2)^2 - \ell_2^2 & = & 0 \end{array} \tag{68}$$

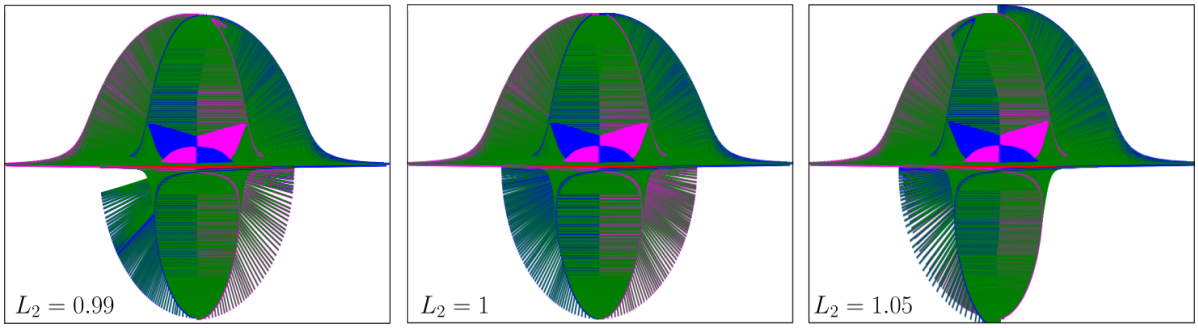

Figure 12: In the workspace, representation of all configurations for the robot, for different values of L_2

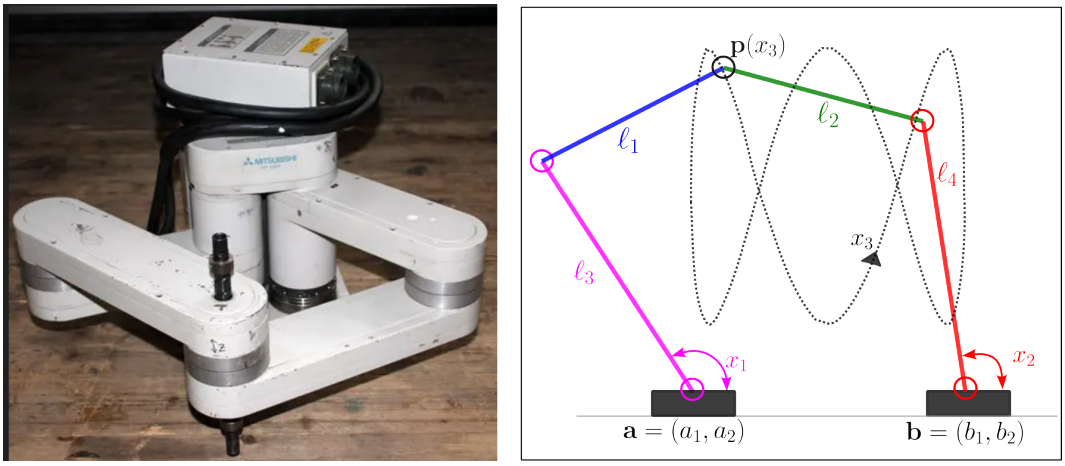

Figure 13: Left: RP-5AH Robot (Courtesy of Mitsubishi Electric Corporation).
Right: The point $\mathbf{p}$ should stay on the Lissajou curve

Using our algorithm for $\varepsilon = 2^{-6}$, in less than 1 sec, we get Figure 14, right, to be compared with the continuation method (left) obtained by [13]. The frame box is taken as

$$[\mathbf{x}] = [-0.6, 2.5] \times [0.7, 2.1] \times [0, 2\pi]. \tag{69}$$

Note that the continuation method is also based on parallelepipeds, but looses solutions (compare carefully the top on the two figures) in some specific situations, where no valid initial points are chosen near the solution curve to be selected.

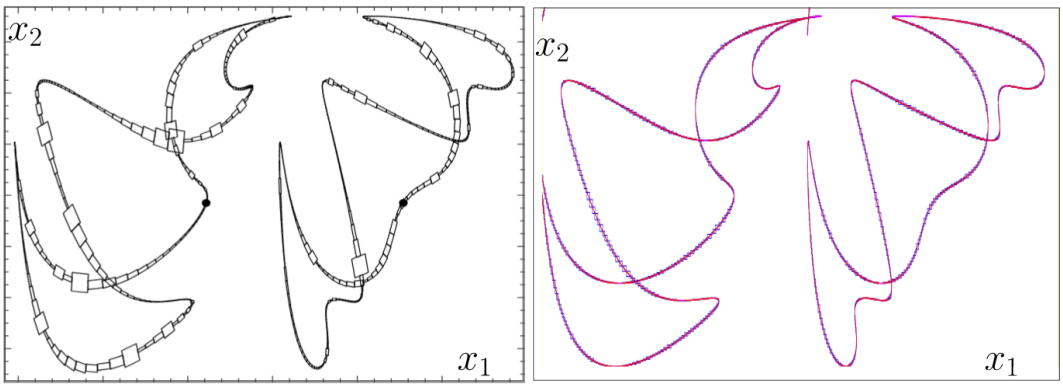

Figure 14: Solution set of the two armed problem in the (x_1, x_2) space;
Left: continuation method, Right: with gutters

In the workspace, a discrete approximation of the occupancy set is depicted on Figure 15.

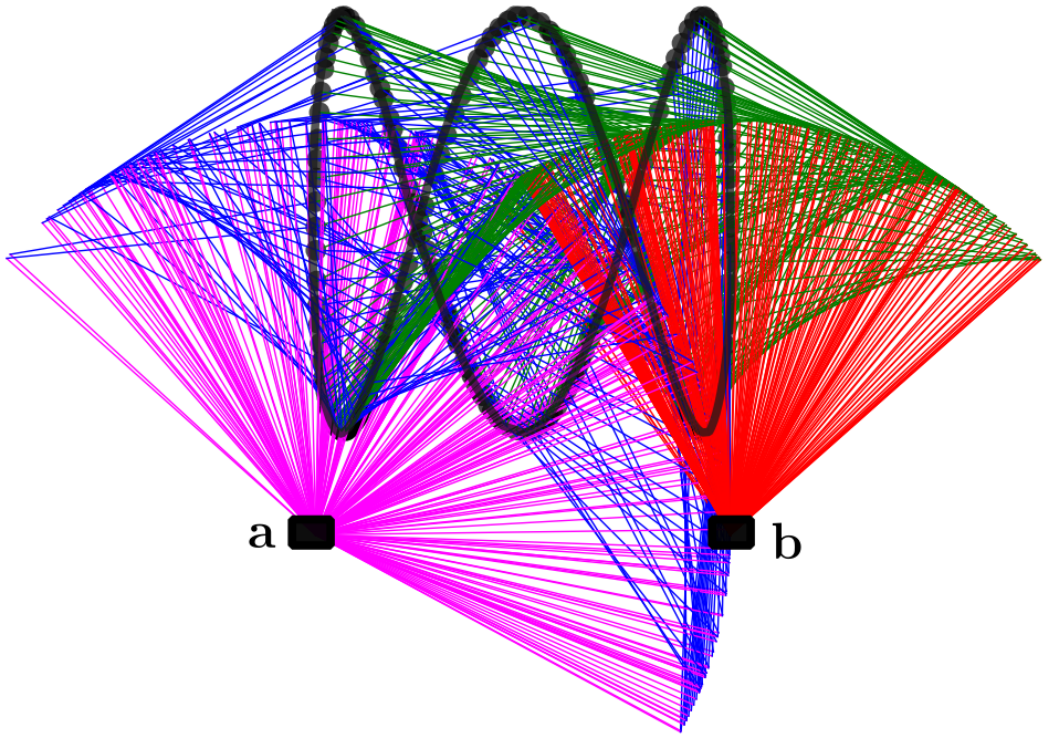

Figure 15: Occupancy set in the workspace

The code source of the test-cases is based on the codac library [19] and can be found at:

https://www.ensta-bretagne.fr/jaulin/buche.html

6 Conclusion

In this paper, we have introduced a new abstract domain called a *gutter* to represent the solution set of a nonlinear equations. A gutter $\langle [\mathbf{x}], \mathbf{A}, \mathbf{b}, \rho \rangle$ is composed of a box $[\mathbf{x}]$, a flat $\mathbf{Ax} + \mathbf{b} = \mathbf{0}$ and a radius ρ.

- The box $[\mathbf{x}]$ is needed to allow nonoverlapping wrappers.
- The flat is needed to have the linear approximation and getting an approximation with an order 1.
- The radius ρ is needed to have the guarantee.

This new wrapper makes it possible to increase the accuracy of the approximation compared to classical interval techniques. Moreover, gutters are easy to project or to intersect, which is not the case for other first order approximations such as parallelotopes, ellipsoids, zonotopes.

Three test-cases taken from the literature have shown the efficiency of gutters and the accuracy of the approximation that could be obtained.

References

[1] M. Arsenault. *Développement et analyse de mécanismes de tenségrité*. PhD thesis, Université Laval, Québec, Canada, 2006. Thèse de doctorat.

[2] M. Berger. *Espaces euclidiens, triangles, cercles et sphères*, volume 2 of *Géométrie*. Cedic/Fernand Nathan, Paris, France, 1979.

[3] C. Combastel. A state bounding observer for uncertain non-linear continuous-time systems based on zonotopes. In *Proceedings of the 44th IEEE Conference on Decision and Control (CDC)*, pages 7228–7234. IEEE, 2005.

[4] P. Cousot and R. Cousot. Abstract interpretation: A unified lattice model for static analysis of programs by construction or approximation of fixpoints. In *Conference Record of the Fourth ACM Symposium on Principles of Programming Languages*, pages 238–252, Los Angeles, California, 1977.

[5] M. Godard, L. Jaulin, and D. Masse. Inner and outer approximation of the image of a set by a nonlinear function. *International Journal of Approximate Reasoning*, 187:109574, 2025.

[6] E. R. Hansen. *Global Optimization using Interval Analysis*. Marcel Dekker, New York, NY, 1992.

[7] M. HladÃk. Enclosures for the solution set of parametric interval linear systems. *International Journal of Applied Mathematics and Computer Science*, 22(3):561–574, 2012.

[8] L. Jaulin. Asymptotically minimal interval contractors based on the centered form. *Acta Cybernetica*, 26(4):933–954, 2024.

[9] L. Jaulin, M. Kieffer, O. Didrit, and E. Walter. *Applied Interval Analysis, with Examples in Parameter and State Estimation, Robust Control and Robotics*. Springer-Verlag, London, 2001.

[10] L. Jaulin and E. Walter. Guaranteed nonlinear estimation and robust stability analysis via set inversion. In *Proceedings of the 2nd European Control Conference*, pages 818–821, 1993.

[11] V. Kreinovich, A.V. Lakeyev, J. Rohn, and P. Kahl. Computational complexity and feasibility of data processing and interval computations. *Reliable Computing*, 4(4):405–409, 1998.

[12] A. Kurzhanski and I. Valyi. *Ellipsoidal Calculus for Estimation and Control*. Birkhäuser, Boston, MA, 1997.

[13] B. Martin, A. Goldsztejn, L. Granvilliers, and C. Jermann. Certified parallelotope continuation for one-manifolds. *SIAM Journal on Numerical Analysis*, 51(6):3373–3401, 2013.

[14] A. Miné. The octagon abstract domain. *Higher Order Symbol. Comput.*, 19(1):31–100, 2006.

[15] R. Moore. *Methods and Applications of Interval Analysis*. Society for Industrial and Applied Mathematics, jan 1979.

[16] H. Ratschek and J. Rokne. *New Computer Methods for Global Optimization*. Ellis Horwood, Chichester, UK, 1988.

[17] A. Rauh and E. Auer. *Modeling, Design, and Simulation of Systems with Uncertainties*. Springer, 2011.

[18] N. Revol. Introduction to the IEEE 1788-2015 Standard for Interval Arithmetic. *10th International Workshop on Numerical Software Verification - NSV 2017*, 2017.

[19] S. Rohou, B. Desrochers, and F. Le Bars. The codac library. *Acta Cybernetica*, 26(4):871–887, 2024.

[20] S. M. Rump. INTLAB - INTerval LABoratory. In Tibor Csendes, editor, *Developments in Reliable Computing*, pages 77–104. Kluwer, Dordrecht, the Netherlands, 1999.

[21] V. Turkulov, M.R. Rapaić, and R. Malti. Stability analysis of time-delay systems in the parametric space. *Automatica*, 157, 2023.

[22] J. Wan. *Computationally reliable approaches of contractive model predictive control for discrete-time systems*. PhD dissertation, Universitat de Girona, Girona, Spain, 2007.

[23] P. Wenger and D. Chablat. Kinetostatic analysis and solution classification of a class of planar tensegrity mechanisms. *Robotica*, 37(7):1214–1224, 2019.